UNIVERSITA' DEGLI STUDI DI GENOVA

FACOLTA' DI INGEGNERIA

BACHELOR'S THESIS

Drag reduction and terminal velocity measurements on superhydrophobic spheres

Supervisor: Alessandro Bottaro, Professor, Department of Civil Engineering, Chemistry and Environmental, University of Genova

Correlator: Nicolas Mazellier, Professor, Polytech Orléans

Student: Luca Cò

July 2015

Abstract

This study was carried out within the Aerodynamics lab of Polytech Orleans.
Its purpose was to evaluate terminal velocity and drag reduction achieved through superhydrophobic coating applied to spheres of metal of 10 mm of diameter falling in a tank with both high and low viscosity liquid.
We used two types of fluids for our experiment: glycerol and water.
After a first introductory chapter regarding superhydrophobic surfaces and its chemical and physical properties, we will present our experiments and experimental lab.
Therefore, we will discuss the post-processing methods and the results achieved.
At last, we move on to deal the environmental impact that superhydrophobic surfaces could have and its future applications.

Index

Index of figures

Index of Tables

1 Introduction to superhydrophobic surfaces

For hydrophobicity we mean the physical property of chemical species (for example molecules) to be rejected by the water.
The term is used as well in a broader sense to indicate the properties of materials of not absorbing and not retain water inside them or on their surface.

We can speak about hydrophobicity in the sense of not wetting water :
A surface is said hydrophobic when a drop of water on its surface forms a contact angle greater than 90 °. In this case the material is commonly said water repellent. If this angle is greater than 150 ° the surface is said superhydrophobic (SH in the following).

In a material the properties of the surface are closely linked to both the chemistry and the topography (micro- and nano-scale). For example the leaves of some plants, most notably the lotus' ones, through a hierarchical structure, are equipped with exceptional SH properties. Taking inspiration from nature, the creation of micro-and nano-asperities on the surfaces metrics is more and more often consciously used to modify in a controlled manner the characteristics of the surfaces. In particular, this technique can make the systems tribology more efficient and respectful of the environment.
Suffice it to say, as an example, the accumulation of microorganisms, plants, etc. on the hull of ships, with a consequent increase up to 40% of the fuel consumption, or in the pipes of the industrial equipment, with considerable loss in efficiency. Normally apply chemicals whose action can be of limited effectiveness and harmful to the environment. Similar reasoning applies to the methods of protection from the lie of the wind turbines, aero wings and electric cables. All this can be effectively replaced by machining micro structured surfaces that simply prevent ice and fouling, essentially thanks to a film of air at the solid-liquid interface (plastron).
Among the properties of the surface, very important for the purposes of tribological problems is the wettability, or the degree of adhesion of a liquid deposited on the surface under examination.

1.1 Wettability , hydrophobicity and superhydrophobicity

Wettability is the ability of a liquid to maintain contact with a solid surface, resulting from intermolecular interactions when the two are brought together. The degree of wettability is determined by a force balance between adhesive and cohesive forces. The first one are due to the attraction between the molecules of the solidus and liquidus and tend to increase the area of interface surface / liquid, flattening the drop.
The cohesive forces, which they tend to minimize the surface, generating a more spherical shape as possible .

Wetting deals with the three phases of materials: gas, liquid, and solid.
In case of a liquid drop resting on a solid surface (as shown in figure below, where the left drop displays an apparent contact angle α smaller that 90 °, whereas a drop deposited onto the same glass sprayed with carbon nanotubes shows a much larger contact angle)

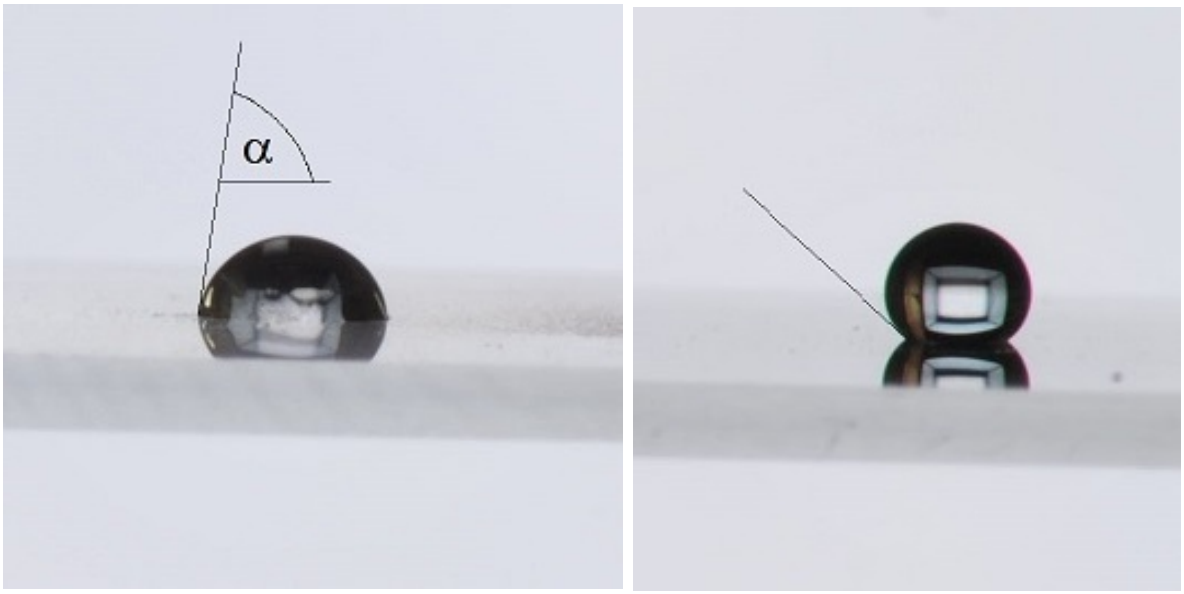

Fig. 1 A small drop of water deposited onto clean glass (left) and onto SH surface (right)

we must consider three values of surface tensions, in correspondence of the three surface existing separations (as shown in Fig.2):

γSG is the surface tension existing on the surface of separation between the solid and the air.
γGL is the surface tension existing on the separation surface between the liquid and the air.
γLS is the surface tension existing on the surface of separation between the liquid and the solid.
γSG is going to expand the drop of liquid on the solid surface; γGL and γLS, or rather their resulting , are going to offset the effect of the first.

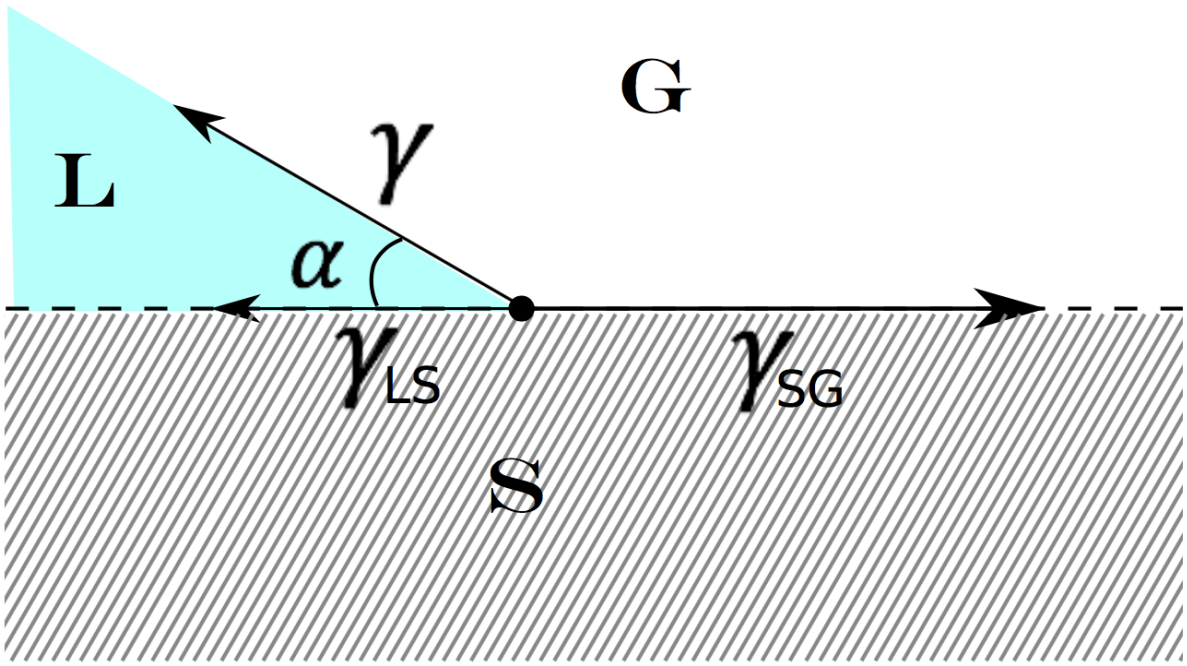

Fig. 2 Static force balance at a triple line.

Considering the Young relation we have:

$$A = \gamma_{SG} - \gamma_{LS} = \gamma_{GL} \cos\alpha$$

Where A is the adhesion tension.

A value of α between 0^o and 90^o (high wettability) means that the liquid is strongly attracted to the solid, which is thus called hydrophilic; when α exceeds 90^o (low wettability) the surface is said to be hydrophobic. When the apparent contact angle exceeds 150^o the surface is called superhydrophobic.

A low-surface-energy material is the first condition for superhydrophobicity. The second condition rests on the roughness or surface topography produced by fabrication and coating processes.

After having spoken about static contact angle, which gives us information on the balance of the surface, in many cases of interest is important that the fluid is able to flow away quickly. It is therefore helpful to consider another factor when speaking about superhydrophobicity: the roll-off angle (Fig.3).

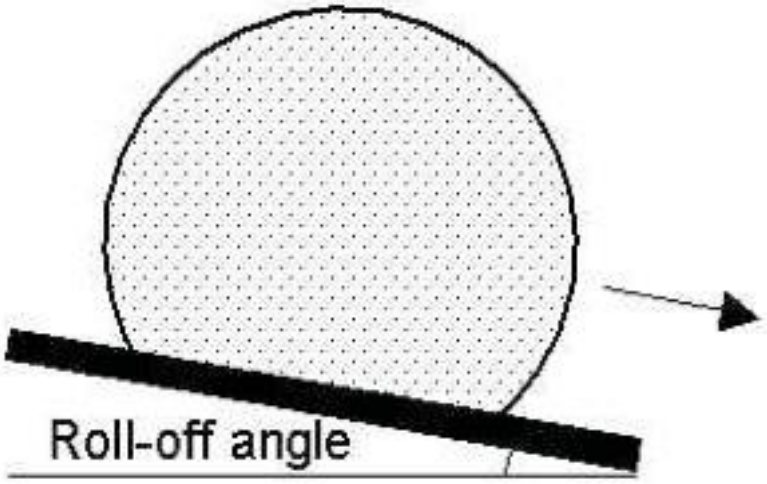

Fig. 3 Roll-off angle

It is the minimum angle at which a surface must be tilted because the drop is able to abut. This measure can be used to classify the surface as well, but the result does not necessarily coincide with those obtained by measuring the contact angle only. Currently, it speaks of SH surface when the static contact angle is around 150 ° and the tilt angle of <10 ° (As shown in picture below).

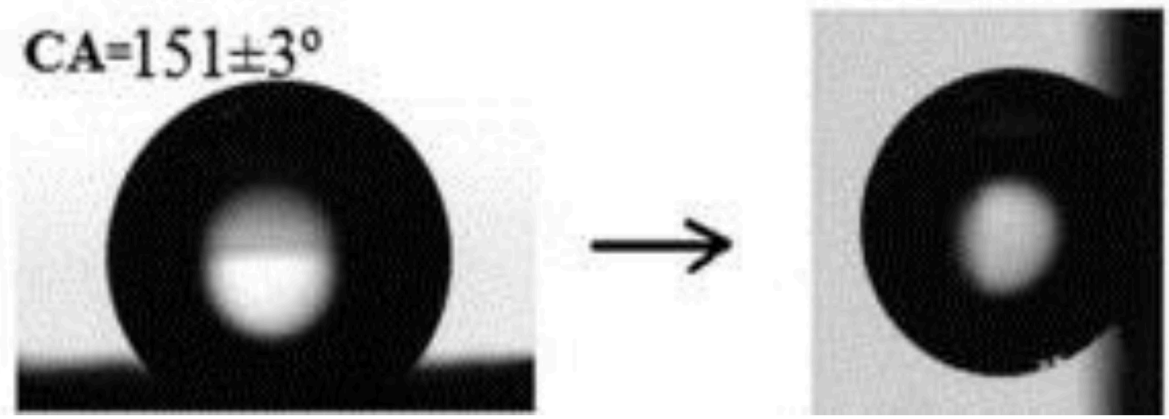

Fig. 4 Static and dynamic angle for a drop on a SH surfaces

The title angle is related to the contact angle hysteresis $\Delta\vartheta$, defined as the difference between the contact angle on the front position, θf, and that in the back, θr, on an inclined surface (Fig.5)

$$\Delta\vartheta = \theta f - \theta r$$

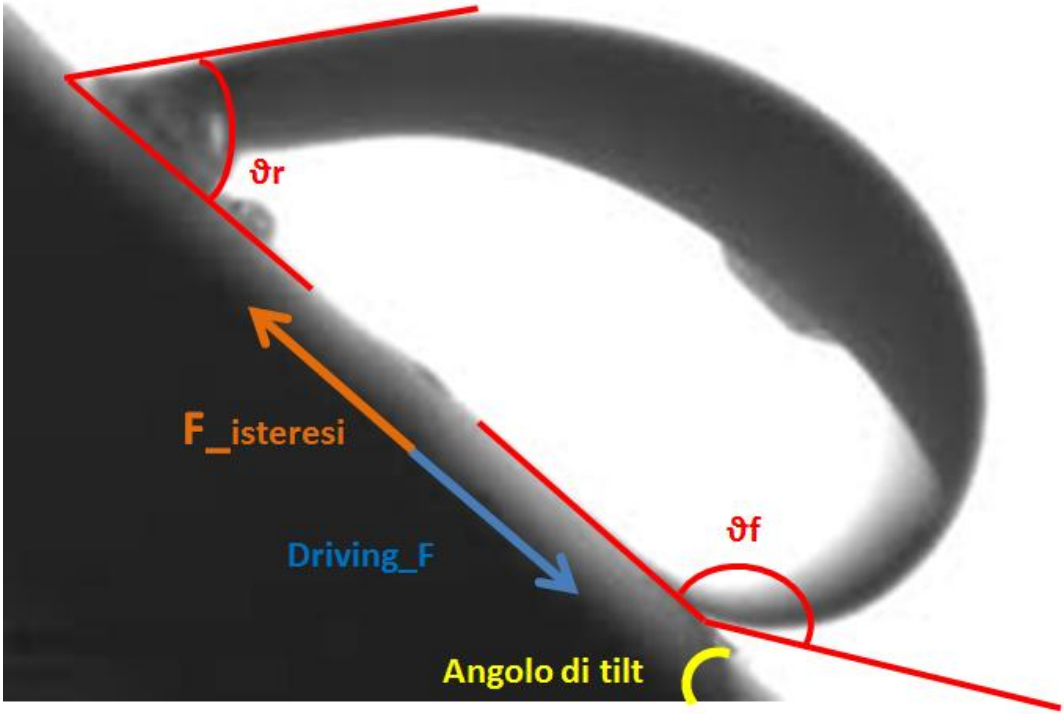

Fig. 5 The contact angle hysteresis

The difference between the two angles is due to the inhomogeneity of the substrate that tend to block the front face of the drop. It generates a curvature gradient which induces in turn a pressure gradient at the interface, inducing a capillary force ("F_isteresi" in Fig.5) opposite to the parallel component of the force of gravity ("driving_F" in Fig.5).
In case of superhydrophobicity, the contact angle is extremely high (150 °), while its hysteresis is drastically low (<10 °). This in cause of the air trapped under the drop "homogenized" the surface of the solid. Thanks to this dual effect ($\theta \rightarrow 180$ °, $\Delta\theta \rightarrow 0$ °) even very small droplets adhere much less than usually happens.
In order to have maximum mobility, we must simultaneously maximizing the contact angle and minimize its hysteresis. From the practical point of view, we can gradually reduce the solid surface interspersing with empty slots of micrometric dimensions. In this way, the contact line touches the surface only on the tips of solid columns. However, there is a physical limit, since there is a maximum static pressure which can be supported by the pillars air (Cassie-Baxter state) beyond which the water penetrates inside the cavities so intimately adhering to the roughness of the solid surface, preventing the mobility (Wenzel state).

1.2 Roughness of the surfaces: Wenzel and Cassie-Baxter theory

As already described above, a low-surface-energy material is the first condition for SH. The contact angle is changed by the roughness of the surface. Typically, on the surface that we consider flat in the macroscopic sense, discrepancies and defect of various kind (chemical or physical) are presents. They are artificially produced in order to modify the wettability (and hence endowed with a certain regularity), both random or inherent to the structure macroscopic material used.
Wenzel was the first to study the wetting characteristics of rough materials.
We can define the surface planar projection of the drop on the geometric plane of the surface, which is the area that appears to be macroscopically wetted the drop. It defines actual surface of the interface the real area of concrete surface really wet drop, while taking account of its roughness. The parameter that describes the ratio between the area and the projected area is the roughness factor: r.
In the Wenzel model the drop of liquid is in contact with all points of the surface below (fig 1.7), then the area is greater than the projected area ($r \geq 1$).

Fig. 6 The Wenzel model

Considering the equilibrium contact angle in the Wenzel state, α_W which is given by : $cos\alpha_W = rcos\alpha$, we can define the effective adhesion tension r A :

$$r\,A = \gamma_{GL}\cos\alpha_W$$

Whereas A depends solely on the chemical composition of the three contiguous phases, the effective adhesion tension varies widely with the microscopic morphology of the solid. the presence of the parameter r indicates that roughness reinforces hydrophobicity (as well as hydrophilicity) with respect to a smooth surface.
Despite criticisms, Wenzel's averaged view represents a useful scheme for uniformly rough surfaces and for drops much larger than the length scale of surface heterogeneities.
One aspect which complicates the understanding of wetting phenomena is the contact angle hysteresis, of which we spoke before.

The asymmetry in contact angles creates a Laplace pressure difference between the front of the drop (high curvature and high pressure) and the rear (small curvature and small pressure) so that the weight of the drop might be balanced. Even in this case chemical heterogeneities and roughness can act as pinning sites, so that the hysteresis $\Delta\vartheta = \theta f - \theta r$ depends strongly on surface properties.
If air is trapped within asperities, so that the solid-liquid contact area is decreased, ultra- or super-hydrophobicity can be attained, with the drop partially sitting on air (this is known as the Cassie-Baxter or fakir state, an example in fig. below).

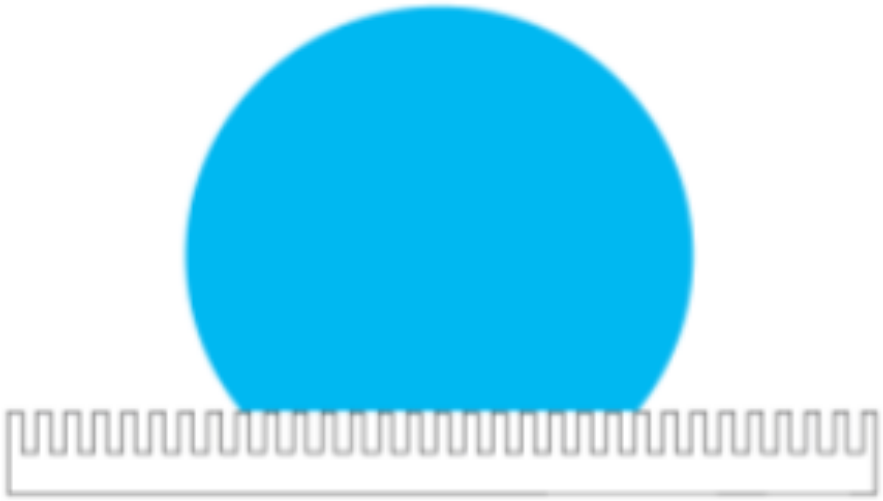

Fig. 7 Cassie and Baxter model

Capturing and maintaining a connected gas layer (or disconnected gas bubbles) between the solid and the liquid depends crucially on the way the solid surface is structured. Cassie & Baxter have proposed the following equation to describe the contact angle α_F in the fakir state:

$$\cos\alpha_F = f_1\cos\alpha - f_2$$

with f_1 the total area of solid per unit projected area under the liquid and f_2 defined in an analogous way for the air-liquid interface (as shown in picture below , Fig.8)

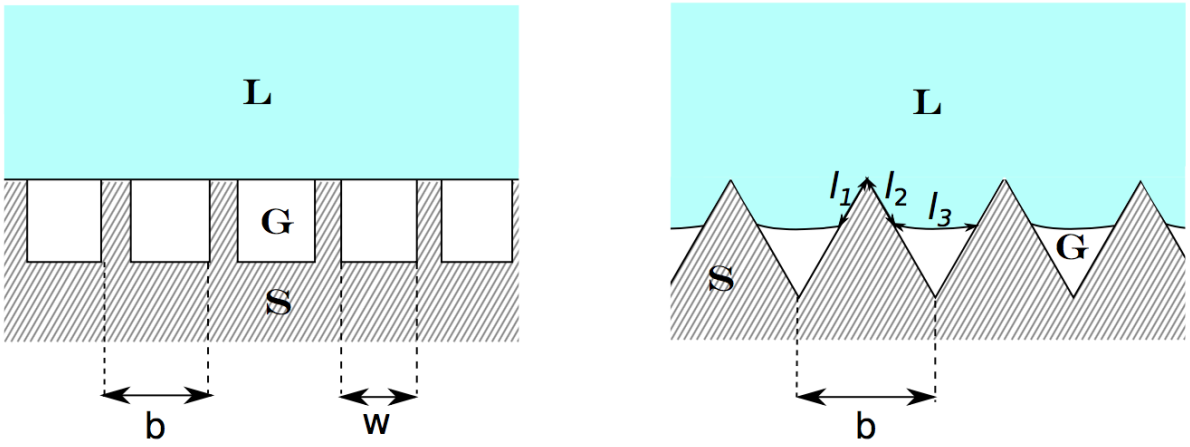

Fig. 8 Close up of two (periodic) rough surfaces, taken to be homogeneous in the third direction. In the left frame, with reference to Cassie-Baxter equation it is $f_1 = 1 - w/b$ *and* $f_2 = w/b$*, whereas in the right frame* $f_1 = (l_1 + l_2)/b$ *and* $f_2 = l_3/b$.

We can note that when the air layer disappears, $f_1 \rightarrow r$ and $f_2 \rightarrow 0$, so that

$\cos \alpha_F = \cos \alpha_W = r \cos \alpha$.

When the solid surface is homogeneous and smooth ($r \rightarrow 1$) it is correctly recovered that

$\alpha_F = \alpha_W = \alpha$.

Then we can consider Wenzel state as a limit of Cassie-Baxter state.

The figure below (1.11) can help us to make clearer the difference between Wenzel state (at the left) and Cassie-Baxter state (at the right)

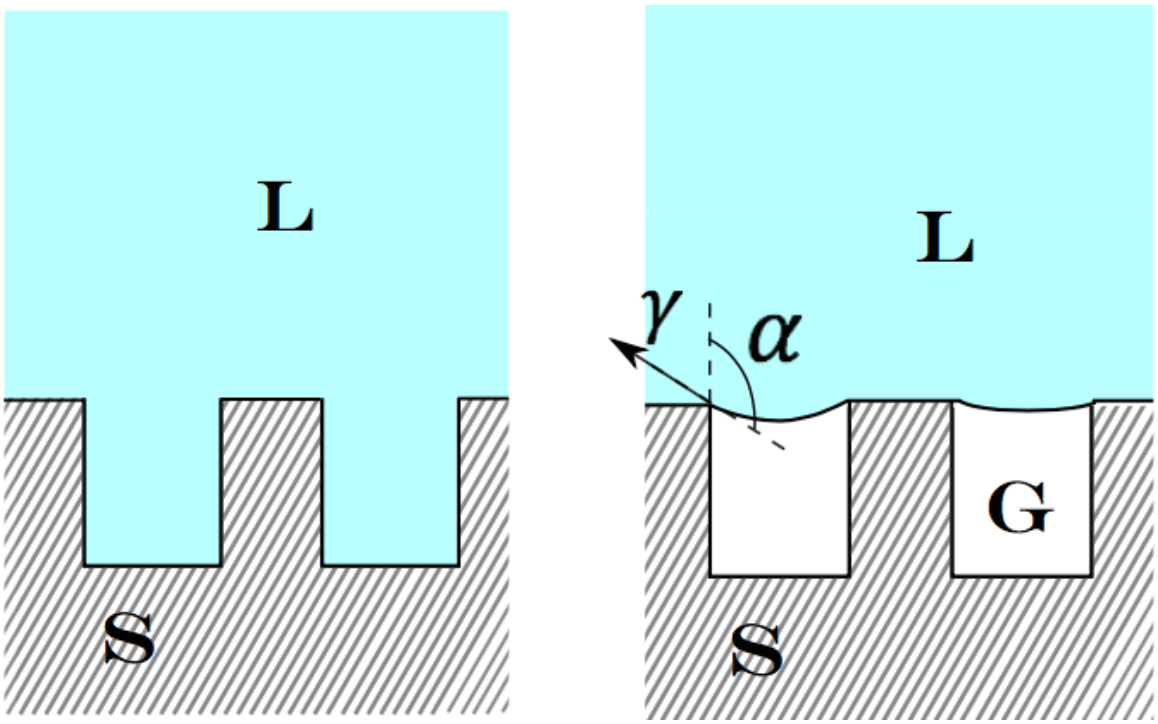

Fig. 9 From left to right : Wenzel state; Cassie-Baxter state

Once it studied the motion of a liquid on a SH surface we can rightly ask what happens instead if a solid with SH surface is in motion into a liquid. This is not a pure scientific curiosity: devices of this type may lead to an enormous energy savings if also in this case the friction proves reduced. First of all it must be considered that in the case of objects in motion in a liquid, the friction is essential between the layers, liquid-liquid that slide over one another more that among solid-liquid (laminar regime in the first layer of the liquid adheres in fact at the solid surface and moves integrally with it).
Second is carefully analyzed the role of the air layer. Whereas the viscosity of the air is less than that of water, it might be considered in fact that the layer of small air bubbles can play a key role in reducing friction between the fluid and the SH surface. This is true in the case of laminar flow (where the thin air layer functions as a lubricant, as well as in the hovercraft) but not in the case of turbulent flow, where paradoxically the SH seems to be counterproductive. The resistance of the air bubbles is in fact due to two components, friction and pressure. The fact that the air viscosity is less than that of water may decrease the first component, but is liable to increase the second up to the point that in the turbulent flows the presence of a layer of air bubbles can be an impediment to the motion. On the other hand, the Laplace pressure variation at the interface due to the curvature of the test surface that the more smaller the radius of curvature of the bubbles and the greater will be the pressure difference on the two faces of the surface of separation between 2 fluid (air / water).
It is therefore not entirely absurd the hypothesis that air functions no longer as a lubricant, but to support and resulting damping of the motion in the fluid.

1.3 Navier slip conditions

The no-slip condition is accepted almost universally as the proper boundary condition to impose at a solid-liquid interface. The concept of a slip boundary condition was first proposed by Navier in 1823 (shown schematically in Fig. 1.12) .
In Navier's model, the magnitude of the slip velocity, u_0, is proportional to the magnitude of the shear rate experienced by the fluid at the wall:

$$u_0 = b \left| \frac{\partial u}{\partial y} \right|$$

where b is the slip length.

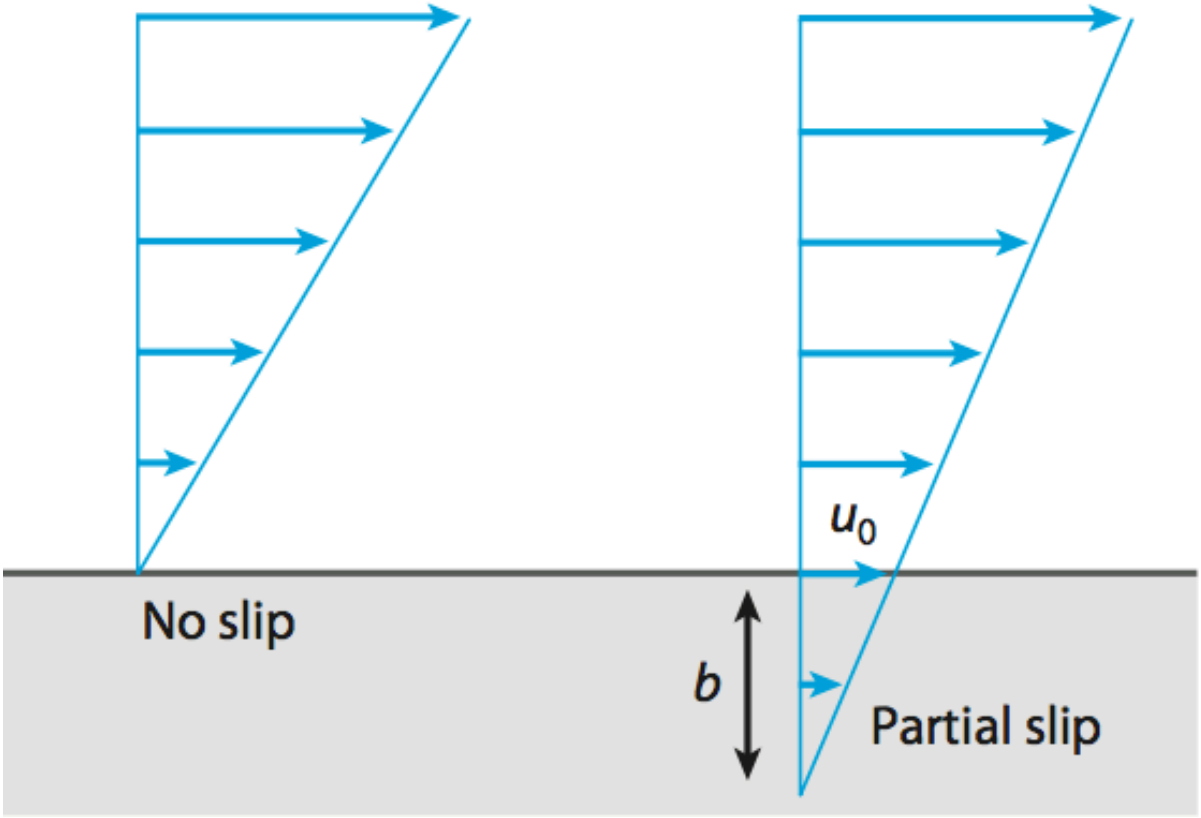

Fig. 10 Schematic diagram of slip at a fluid-solid interface.

The classical no-slip condition is recovered for b = 0 and perfect slip is found for b → ∞.

Speaking in light of Stokes (or creeping) flow (Re < 1), then with very slow fluid velocities (U) and very large viscosities (μ), focusing our attenction on the drag force (Fd) acting on a sphere of radius a, we have:

$$Fd = 6 \pi \mu U a$$

Regarding a SH surface, according to Abraham et al. We will have a drag force of:

$$Fd = 6 \pi \mu U a [(1+ 2b/a) / (1+3b/a)]$$

In case of a short slip lenght (b<< a), according to Taylor and focusing only on the last term of SH drag force *(1+ 2b/a) / (1+3b/a)*, we can consider 3b/a an ε, and then it can be consider equal to
1-b/a, with a resulting drag force of:

$$Fd = 6 \pi \mu U a (1-b/a)$$

It is important, then, to have a slip length large enough, in order to be able to have an high drag force reducing. In the following chapter we will briefly discuss on it and on methods to make SH the surfaces, through painture or not, and its duration and resistance to external agents.

2 State of the art on superhydrophobic surfaces

Summarizing what it is written above, the SH surfaces can bring advantages both in the reduction of drag force (for bodies moving in a fluid) both in increasing the water resistance and decrease the wettability of the surfaces. It is seen that they have also positive effects in reducing the fouling (see chapter 6 for further explanation).
Regarding the methods to fabricate the non-wettable surfaces, all based on combining a low-surface-energy material with a rough surface morphology. Materials of choice for designing, developing and producing SH surfaces are polymers; they are versatile, have excellent surface properties and can be easily formed.
In the context of laboratory experiments, SH surfaces are often realized using microfabrication processes developed for the electronic industry. The issue related to this method is the prohibitively expensive cost, which doesn't permit a large-scale manufacturing. There is a low cost alternative to this, which consist in the one-step casting technique with a membrane filter as the mold. In the former study, a disordered array of poly(dimethyl)siloxane micro-pillars hinged on a substrate of the same material was achieved.
In the latter, polycarbonate hairs were cast on a polypropylene substrate. The limitation of this casting approach lies at present in the little resistance of the fibrous structures to abrasion, and the difficulty of producing large scale samples, for example for naval applications.
Another alternative is constituted by spray deposition (the technique used by us in our experiments), which allows to rapidly and conformally coat large areas on a variety of substrates.
Generally, The biggest problem of SH surfaces is related to the longevity of the Cassie-Baxter state, when the SH surface is subject to external pressure and shear. Until now, longevity of laboratory-developed coatings is of the order of a few days; this duration has to be extended by a factor of 100 and more, in order to render the technique of interest to the naval industry, otherwise a dewetting strategy might be indispensable. A new anti-fouling paint developed by the company Nippon Paint Marine (http://nipponpaint-marine.com/en/products/a_lf_sea/index.html)
seems to meet some industrial expectations, but care is needed not to interpret marketing boasts as reliable laboratory results. It is probably advantageous to use hydrophilic patches on top of the micro- roughness elements (on those parts in direct contact with the liquid) to pin and stabilize the air-water interface and use an active dewetting system, in order to Maintaining the gas layer which is crucial to inhibit biofouling activity and metal surface corrosion, thanks to the reduced areas of contact between the solid surface and water.

3 Experimental set-up

The experiment that we are about to illutrate,which rappresents the heart of the thesis, sets his goal in verifing the effect of the SH coating applied to bodies moving in a fluid.
The bodies that we have covered are high precision spheres, commercially available, with a nominal diameters of 10mm ± 13 μm and typical masses of 4.034 grams (4,035 with SH coating).
To cover these spheres we used a SH coating produced by "Ultra Ever Dr®y". More accurately, we used the paint "bottom coating®" as a first coating, in order to improve the adhesion of the real SH painture, the "top coating®" (Both are shown in figure 11).
For those interested in buying it, you may relate to the follwing web site :
http://www.ultraeverdrystore.com .
It could also be interesting check the following videos, produced by"Ultra Ever Dry®": that well illustrate the static properties of the coating paint":

- https://www.youtube.com/watch?v=IPM8OR6W6WE
- https://www.youtube.com/watch?v=BvTkefJHfC0

Fig. 11 From left to the right: Bottom coat and Top coat.

In the picture below you may see the spheres already covered (in this exemple we have a setting of varius diameter, not just the 10 mm ones) .

Fig. 12 SH spheres

Both 10 mm spheres, SH and not, were dropped in a transparent plexigass tank with a square base (of 0.1 m per side) tall 0.6 meters. For our measurements, in order to not have any bottom effect and to make it as realistic as possible, we started to calculate the sphere's velocity from h=0 up to h=0,45 meters.
As liquid for the falls we used both glycerol and water, whose properties are fully described in the next chapter.
Here below are illustrated the laboratory and all components that we have applied to realize our experiment.

3.1 Laboratory

The Aerodynamic Lab, which is the laboratory we have been hosted in to make this experience, is located in the "Hall Carnot" which is part of Polytech Orleans, in the city of Orleans (FR).
To be able to achieve our goal, that is to know the exact velocity of the spheres for the all fallen time, we have built and organized the Lab in the way shown in the figure below :

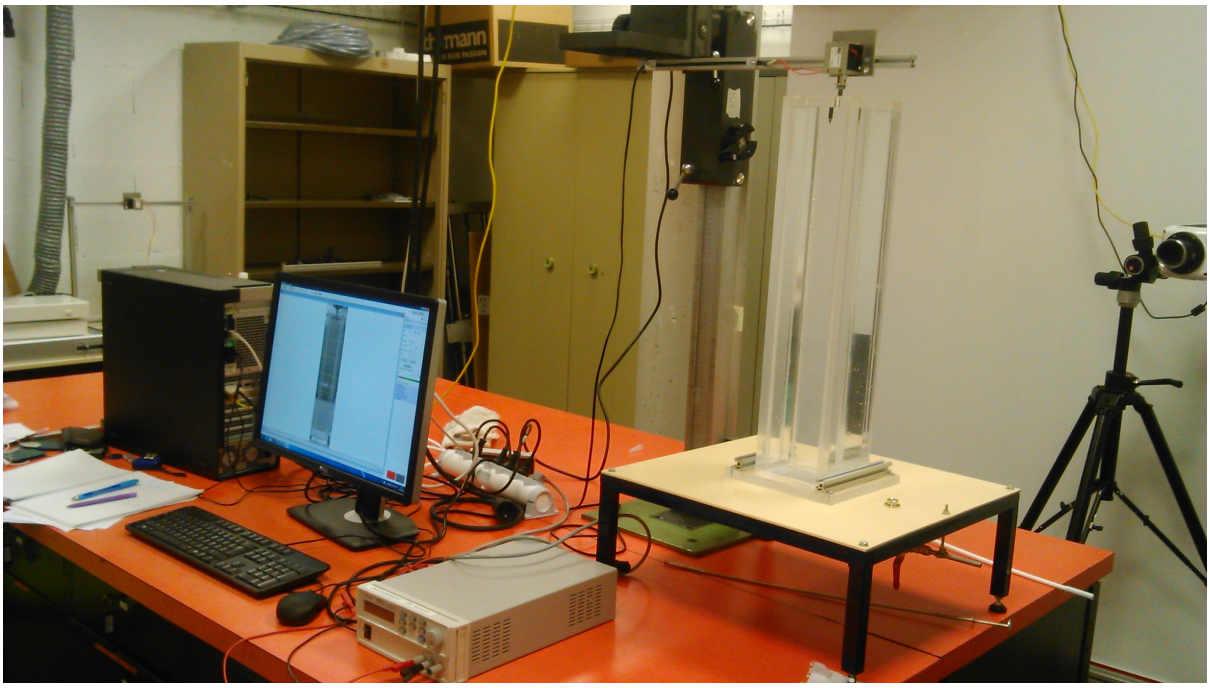

Fig. 13 Laboratory

To register the videos we used a camera produced by Phantom®, model V341 (Fig.14), with a maximum resolution of 2560 x 1600 and 8 Gb of RAM, capable to register until 800 images per second.
This camera was situated at a height of 1,35 m from the ground and always 1,35 m from the tank , facing the front of it.

Fig. 14 Camera

The tank mesured an height from the ground of 1,10 meters.
In order to create a contrast in color as wide as possible, resulting in an higher quality picture resolution, we have placed a great source of light in the back of the cilinder, the lamp used is produced by Just Normlicht®, model Just Daylight 5000 prographic 36w of size 123 cm x 38 cm. The setting is showned in Fig. 15

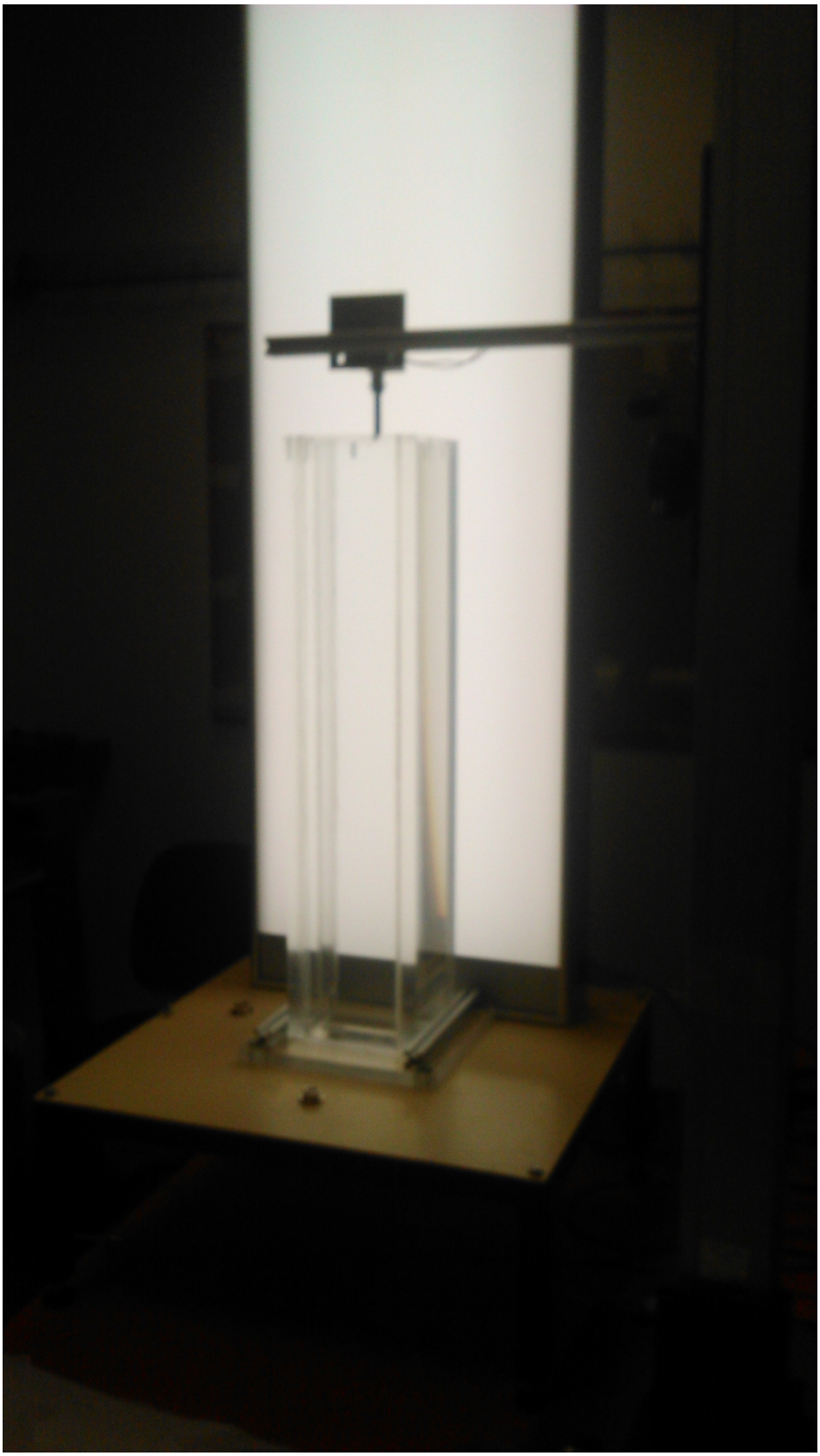

Fig. 15 Laboratory conditions for videos registration.

Thanks to the materials already available in the Lab, we built an apparatus to let the sphere fall. It has function due to a magnetic field generated by a voltage generator produced by Agilent®, model U8001A.
The presence of this magnetic field allows the ball to remain attached to the metal niddled screw located just below the surface of the liquid (Fig. 16), once the voltage generator has been switched off and the magnetic field has been disconnected, the sphere falls under the only effect of its weight.
The value of the voltage generated depends on the required magnetic field and then by the weight of the sphere.

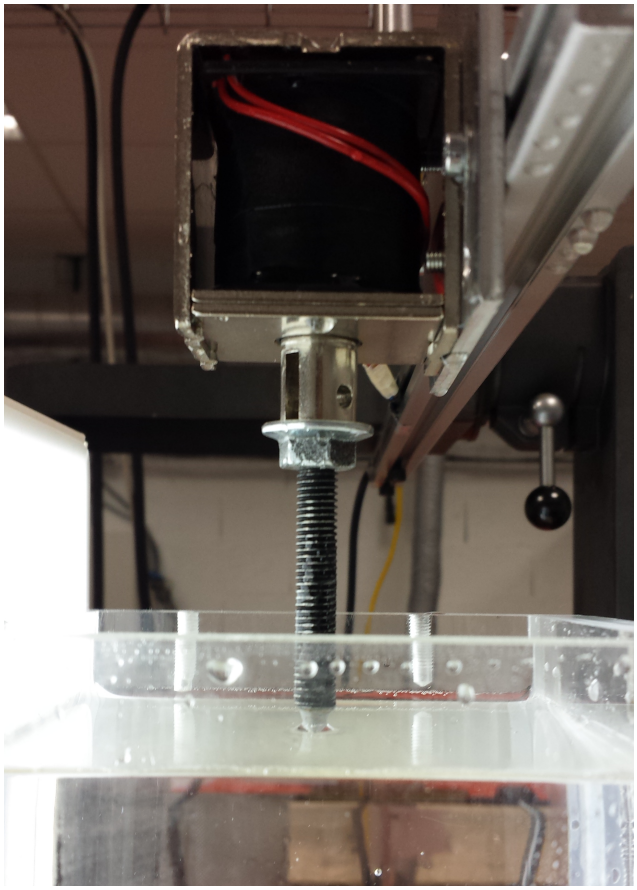

Fig. 16 Apparatus to let the sphere fall

As PC we used a DELL® Precision, model TOWER 5810, with CPU directly connected to the camera. We operated with Windows 7® as software and, most important, we used Matlab R2012a® as program to compute our videos (see the following chapter for further informations regarding it).

It is important to underline that to minimize the contribution of light from other possible sources, experiments have been made with all the lights in the laboratory turned off and windows closed, as to prevent the natural light to penetrate inside.
So the only source of light that the camera sees was the one produced by our light screen (Just Normlicht).
Before passing to the acquisition of our measurements, we made a calibration of each fluid in order to have an accurate conversion between pixels and mm from the point of view of the camera.
It is a very important parameter (for actual results and validity of experiment) during the post processing of data because each fluid has its own refractive index.
We made preliminary tests which have allowed us to put in place the necessary settings for the best use of the camera.

3.2 Process to coat the sphere

What apparently was supposed to be an easy step, it has proved to be quite complicated. This due to the homogeneity of the coating which should be as accurate as possible and the sphere need to be covered all around itself.
As we already told, the paint we used is produced by Ultra Ever Dry® and it uses the technique of nanotechnology to create an air barrier on the surface of the covered object, in order to make that SH. This paint is applied in two different stages: First it must be applied the "Bottom coat" and, after waiting at least 50 minutes, we have applied the "Top coat" and waited further 45 minutes, to complete the process and to achieve a new SH object ready to be used.
To coat the spheres we have identified two possible ways: coating by spray and coating by dipping.
In order to coat them in the best way, balancing both the homogeneity and the full coat, we decided to follow the coating by dipping:
Thus, we dipped the spheres in a clear glass vase containing the"Bottom coat" and waited 1 hour and half to make it dry, and after we repeated the same process another time. Then we did the same thing in a vase full of "Top coat" and waited for 1 hour. After, the spheres were ready.
Is important to remark that in all these passages we have covered ourselves carefully, being these paints and theirs fumes highly toxic.

4 Measurements, post processing and results

4.1 Sphere, liquids and measurements

For this experiment we used several metallic spheres, all of 10 mm of diameter, falling in two liquids, glycerol and water.
In the table below are shown the characteristics of the spheres we have used:

Density [kg/m^3]	7704,37
Radius = **a** [m]	0,005
Crossing Area = **π a^2** [m^2]	0,0000785
Volume [m^3]	5,23598E-07

Tab. 1

We measured personally the density , the dynamic and the kinematic viscosity for both glycerol and water. They have been measured in the Lab of Polytech Orleans using the Stabinger® Viscometer TM SVM 3000, which gave us the following results:

	Glycerol	**Water**
Density [kg/m^3]	1252,8	997,13
Dynamic viscosity [Pa s]	1,0419	0,000891
Kinematic viscosity [m^2/s]	0,000831657	8,93565e-07

Tab. 2

Speaking about the reached velocities, having a maximum length of measurement, gave by the tall of the tank, of 0.45 meters, we achieved the velocities shown in the following figures (from 17 to 20)

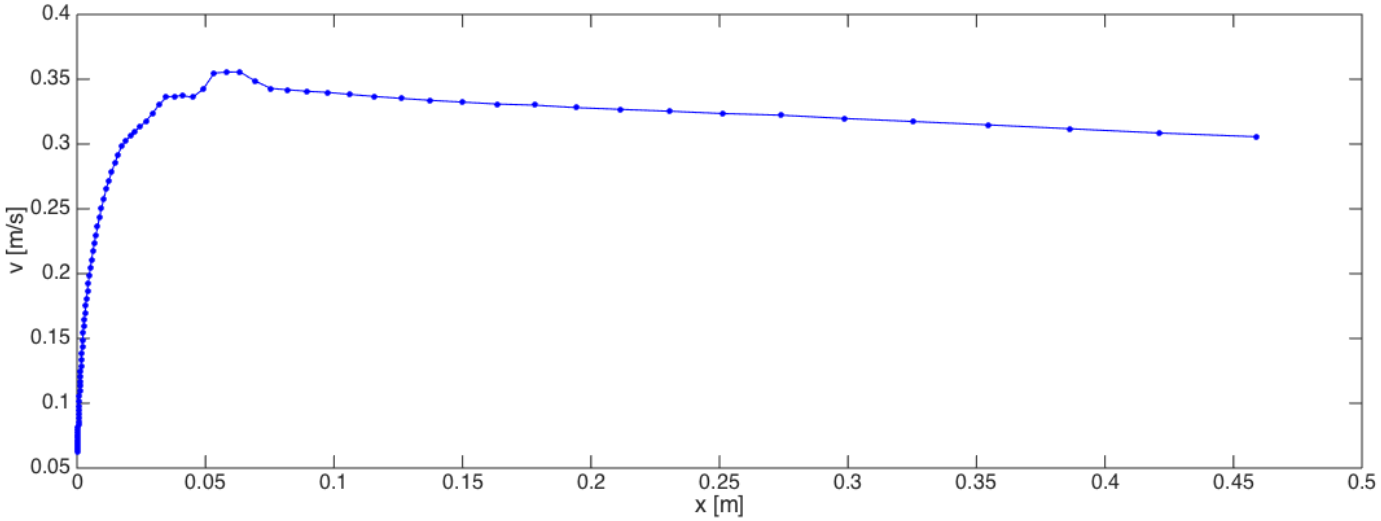

Fig. 17 Sphere uncovered falling into the glycerol

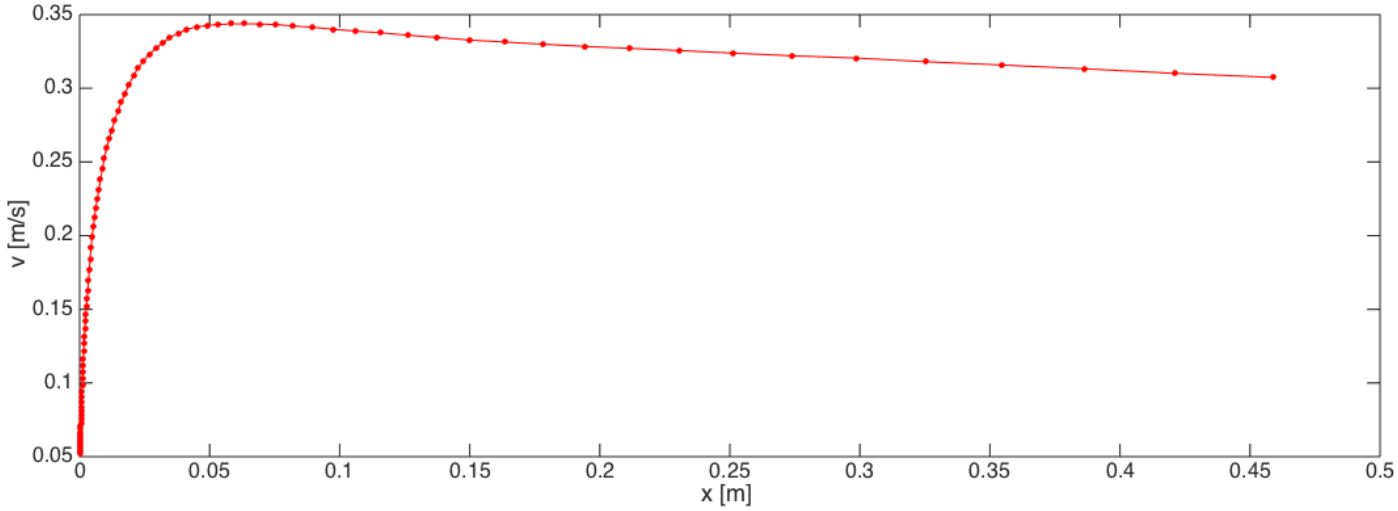

Fig. 18 SH sphere falling into the glycerol

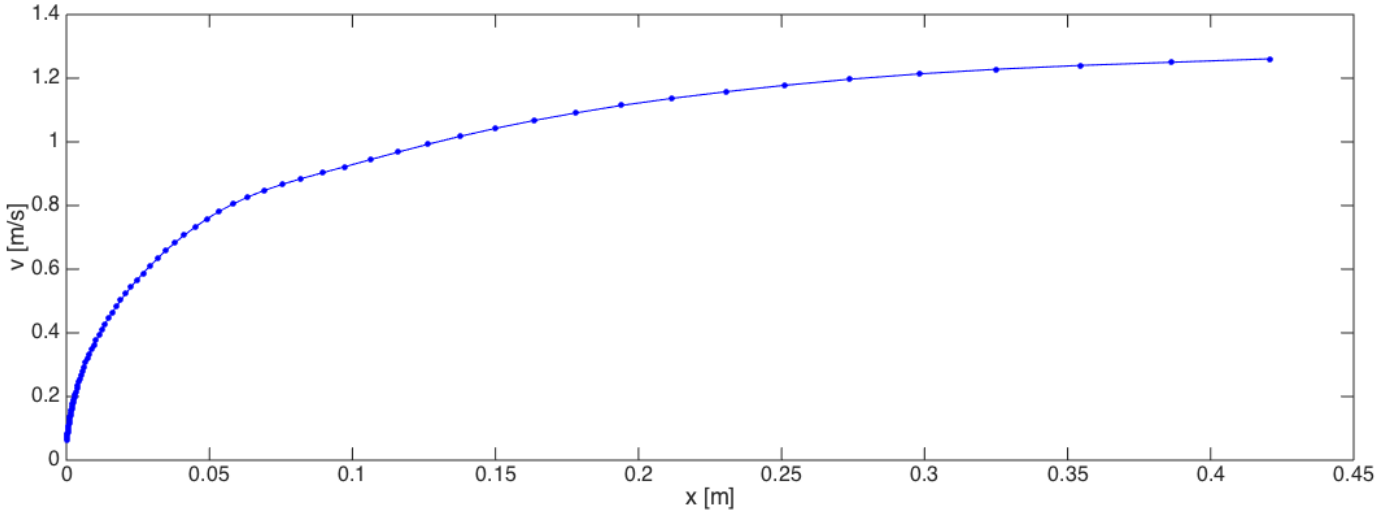

Fig. 19 Sphere uncovered falling into the water

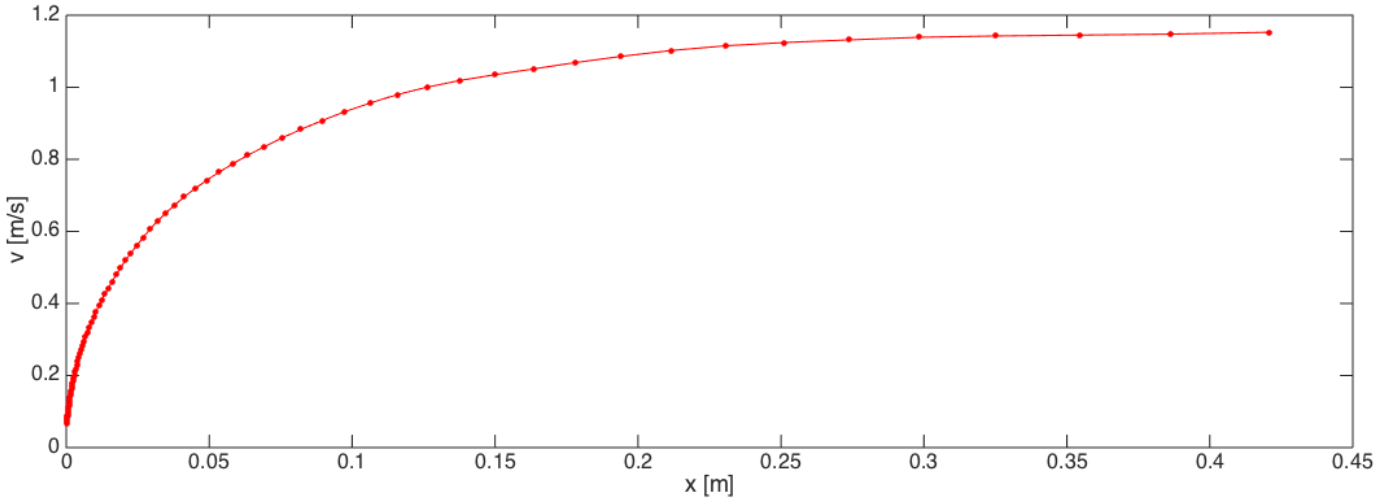

Fig. 20 SH sphere falling into the water

The following table shows us the exact terminal velocity related with their respective Re number, for both spheres SH and not, respectively falling in glycerol and water.

	Glycerol		**Water**	
	Velocity [m/s]	Re	Velocity [m/s]	Re
Uncoated	0,3057	3,675793838	1,261	14112,01942
SH	0,3074	3,696234955	1,153	12903,37699

Tab. 3

We can see as , in the glycerol, the increment is very low, and, on the other hand, how in the water, the coated one becomes harmful.
In the figures below is possible to see exactly the differences between the velocity trend in glycerol and water .

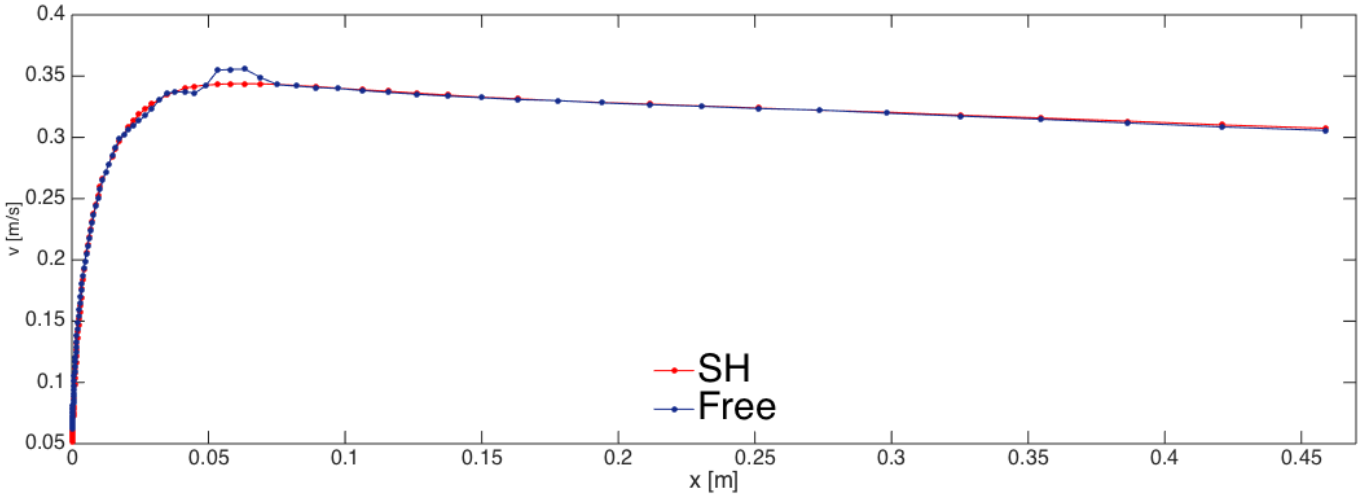

Fig. 21 Overlap of SH coated and uncoated into the glycerol

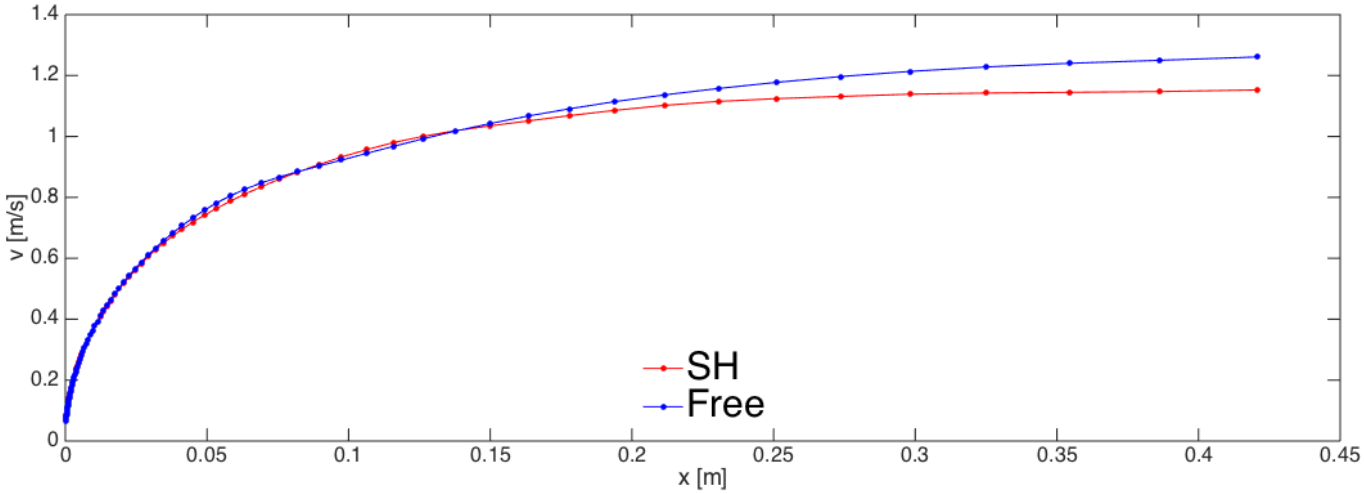

Fig. 22 overlap of SH coated and uncoated into the water

As we can see, the effects we found with both the falls, are not exactly the ones we expected. We will discuss about them in the chapter 5th.

4.2 From movie to images

The results of which we spoke above, and the conclusions that we will comment later on, have been achieved starting from the movies shooted by the camera, described in the third chapter and then computed with Matlab®.
After having recorded the movie, we saved it frame by frame in the file format .tif, cutting of the unecessary ones.
As we did so (usually the number of the pictures we had was around 450, proceeding by saving frame by frame for the falling into the water and further 450 frames, but analized by group of 10 by 10, for the falling in glycerol, due to the low velocities and the incrising time in compliting the trajectory), we started with the computation.

4.3 Computation

4.3.1 Subtracting the background

In order to modify the images saved in .tif format to be able to subtract the background , achieving the results and the changes shown in fig below (23), we used the following Matlab® script:

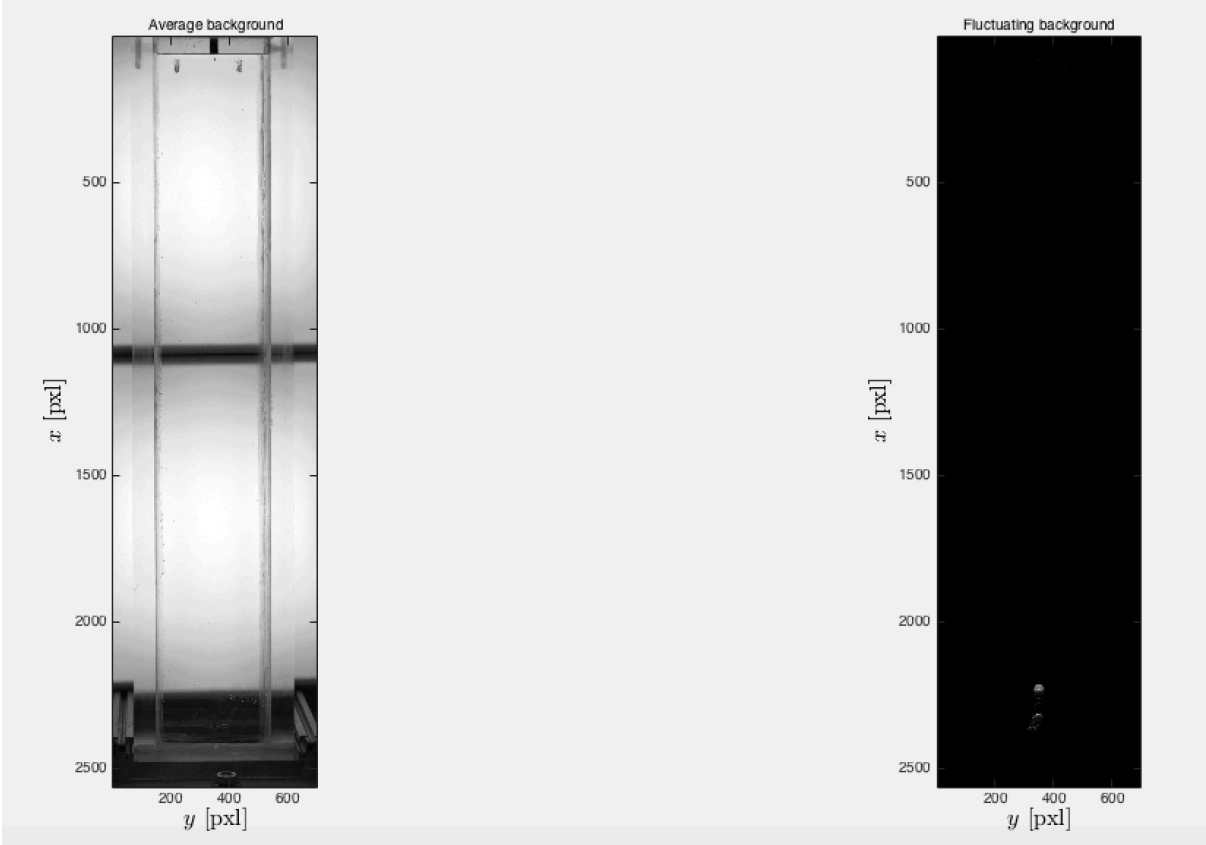

Fig. 23 Average and fluctuating background

```
% Program computing the background image to be subtracted to the falling
% images.
%
% Date: 29/04/2015 (author: Nicolas Mazellier, Luca Co & Adelphe Clepin)
%%%%%%%%%%%%%%%%%%%%%%%%%%%%%%%%%%%%%%%%%%%%%%%%%%%%%%%%%%%%%%%%%%%%%%%%%%%

%%%%%%%%%%%%%%%%%%%%%%%%%%%%%%%%%%%%%%%%%%%%%%%%%%%% Calling of parameters
load('Parameters.mat', 'NbImageNoise', 'Xresolution', 'Yresolution');

%%%%%%%%%%%%%%%%%%%%%%%%%%%%%%%%%%%%%%%%%%%%%%%%%%%% Average Background computation
%Average image initialization
BackgroundAverage = zeros(Xresolution, Yresolution);

h = waitbar(0,'Average background computation: please wait...');
for indIm = 1 : NbImageNoise
    file2read = sprintf('Background/BackImg/Back%.5d.tif', indIm);
    tmp = double(imread(file2read)); % i'm reading this image
    BackgroundAverage = BackgroundAverage + tmp/NbImageNoise;
    waitbar(indIm / NbImageNoise);
end
close(h);

%%%%%%%%%%%%%%%%%%%%%%%%%%%%%%%%%%%%%%%%%%%%%%%%%%%% Fluctuating Background computation
BackgroundVariance = zeros(Xresolution, Yresolution); %Image variance
initialization

h = waitbar(0,'Fluctuating background computation: please wait...');
for indIm = 1 : NbImageNoise
    file2read = sprintf('Background/BackImg/Back%.5d.tif', indIm);
    tmp = double(imread(file2read));
    BackgroundVariance = BackgroundVariance + ((tmp -
BackgroundAverage).^2)/NbImageNoise;
    waitbar(indIm / NbImageNoise);
end
close(h);

%%%%%%%%%%%%%%%%%%%%%%%%%%%%%%%%%%%%%%%%%%%%%%%%%%%%%%%%%%%%%%%%%%%%%%%%%%%
%%%%%%%%%%%%%%%%%%%%%%%%%%%%%%%%%%%%%%%%%%%%%%%%%%%% Results plotting & saving
save('Background/Background.mat', 'BackgroundAverage',
'BackgroundVariance');

figure;
subplot(121);
imagesc(BackgroundAverage)
title('Average background');
colormap(gray) % To change the colours and the landscape
axis image
xlabel('$y$ [pxl]', 'interpreter', 'latex', 'FontSize', 16)
ylabel('$x$ [pxl]', 'interpreter', 'latex', 'FontSize', 16)
subplot(122);
imagesc(BackgroundVariance)
title('Fluctuating background');
colormap(gray) % To change the colours and the landscape
axis image
xlabel('$y$ [pxl]', 'interpreter', 'latex', 'FontSize', 16)
ylabel('$x$ [pxl]', 'interpreter', 'latex', 'FontSize', 16)

clear all;
```

4.3.2 Image denoising

We used the following Matlab® script after having obtained an image in gray scale, and in order to change it in a binary image with the purpose to obtain images with a black background and a white sphere, obtaining a maximum definited shapes (and then areas), as shown in figure below (4.2)

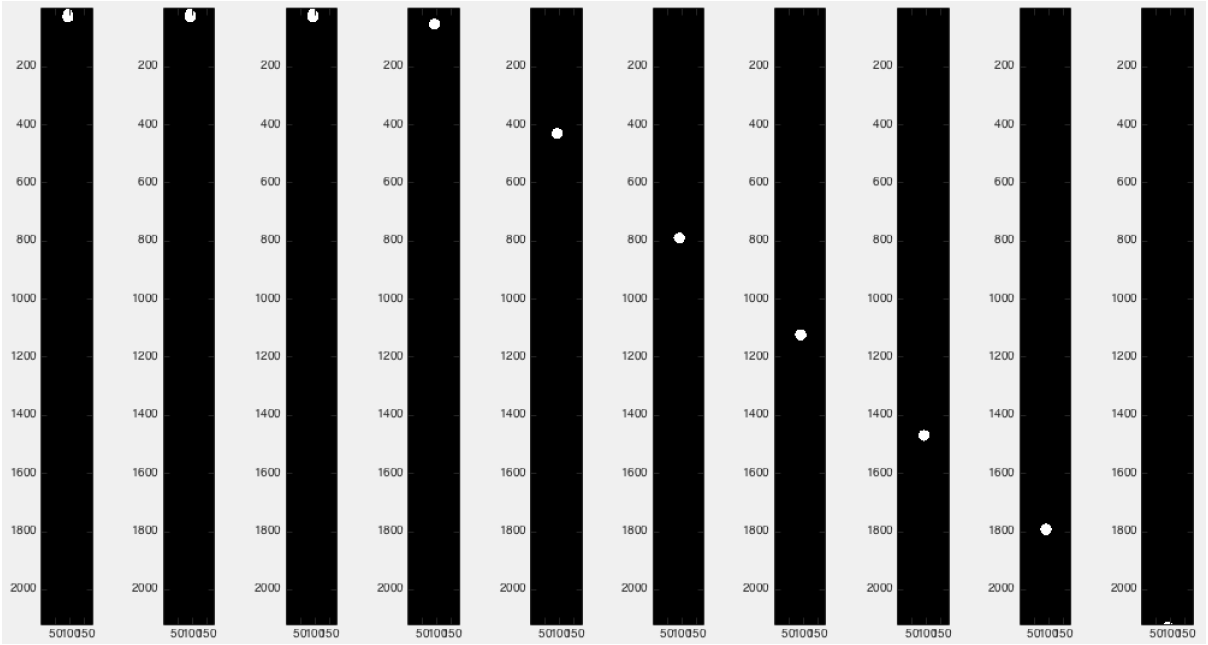

Fig. 24 White sphere on black background

:

```
%%%%%%%%%%%%%%%%%%%%%%%%%%%%%%%%%%%%%%%%%%%%%%%%%%%%%%%%%%%%%%%%%%%%%%%%%%%%
% Program to process images of falling sphere from grayscale to binary
% images.
%
% Date: 29/04/2015 (author: Nicolas Mazellier, Luca Co & Adelphe Clepin)
%%%%%%%%%%%%%%%%%%%%%%%%%%%%%%%%%%%%%%%%%%%%%%%%%%%%%%%%%%%%%%%%%%%%%%%%%%%%

%%%%%%%%%%%%%%%%%%%%%%%%%%%%%%%%%%%%%%%%%%%%%%%%%%%%%%%% Calling of parameters
load('Parameters.mat');

%%%%%%%%%%%%%%%%%%%%%%%%%%%%%%%%%%%%%%%%%%%%%%%%%%%%%%%% Calling of background average image
load('Background/Background.mat', 'BackgroundAverage');

%%%%%%%%%%%%%%%%%%%%%%%%%%%%%%%%%%%%%%%%%%%%%%%%%%%%%%%% Average Background computation
h = waitbar(0,'Image processing: please wait...');
for indIm = 1 : NbImageFall
    %%%%%%%%%%%%%%%%%%%%%%%%%%%%%%%%%%%%%%%%%%%%%%%%%%%%%%%%%%%%%%%%%%%%%%%%%%% Image reading
    file2read = sprintf('Fall/FallImg/Fall%.5d.tif', indIm);
    tmp = double(imread(file2read));
    %%%%%%%%%%%%%%%%%%%%%%%%%%%%%%%%%%%%%%%%%%%%%%%%%%%%%%%%%%%%%%%%%%%%%%%%%%% Background substracting
    tmp = -tmp + BackgroundAverage;
    %%%%%%%%%%%%%%%%%%%%%%%%%%%%%%%%%%%%%%%%%%%%%%%%%%%%%%%%%%%%%%%%%%%%%%%%%%% Cutting
    tmp = tmp(Xindexmin:Xindexmax, Yindexmin:Yindexmax);
    tmp = mat2gray(tmp);
    %%%%%%%%%%%%%%%%%%%%%%%%%%%%%%%%%%%%%%%%%%%%%%%%%%%%%%%%%%%%%%%%%%%%%%%%%%% Convertion in black and white
    [I, J] = find(tmp>=Treshold);
    BWImage = zeros(size(tmp));
    for n = 1 : length(I)
        BWImage(I(n), J(n)) = 1;
    end
    BWImage = bwareaopen(BWImage, BubbleTreshold);
    %%%%%%%%%%%%%%%%%%%%%%%%%%%%%%%%%%%%%%%%%%%%%%%%%%%%%%%%%%%%%%%%%%%%%%%%%%% Saving
    file2save = sprintf('Fall/BWImage/Fall%.5d.mat',indIm);
    save(file2save,'BWImage');
    waitbar(indIm / NbImageFall);
end
close(h);

figure
NbImShow = 10;
indImShow = round(linspace(1, NbImageFall, NbImShow));
for n = 1 : NbImShow
    subplot(1, 11, n)
    file2read = sprintf('Fall/BWImage/Fall%.5d.mat',indImShow(n));
    load(file2read);
    imagesc(BWImage);
    colormap(gray) % To change the colours and the landscape
    axis image % to modify the aspect ratio
end

clear all;
```

4.3.3 Trajectories, velocities and acceleration of the spheres

To be able to pass from the frame by frame falling of the sphere, to know its trajectory and then its velocity, we first have had to calculate the center of our sphere. As we did so, we started to calculate the displacing of the center, frame by frame, knowing the time in between them and that a pixel was equal to 2.479E-4 mm for both glycerol and water.
In the figure below we can see the center of the sphere and its trajectory (regarding a sphere falling into the glycerol)

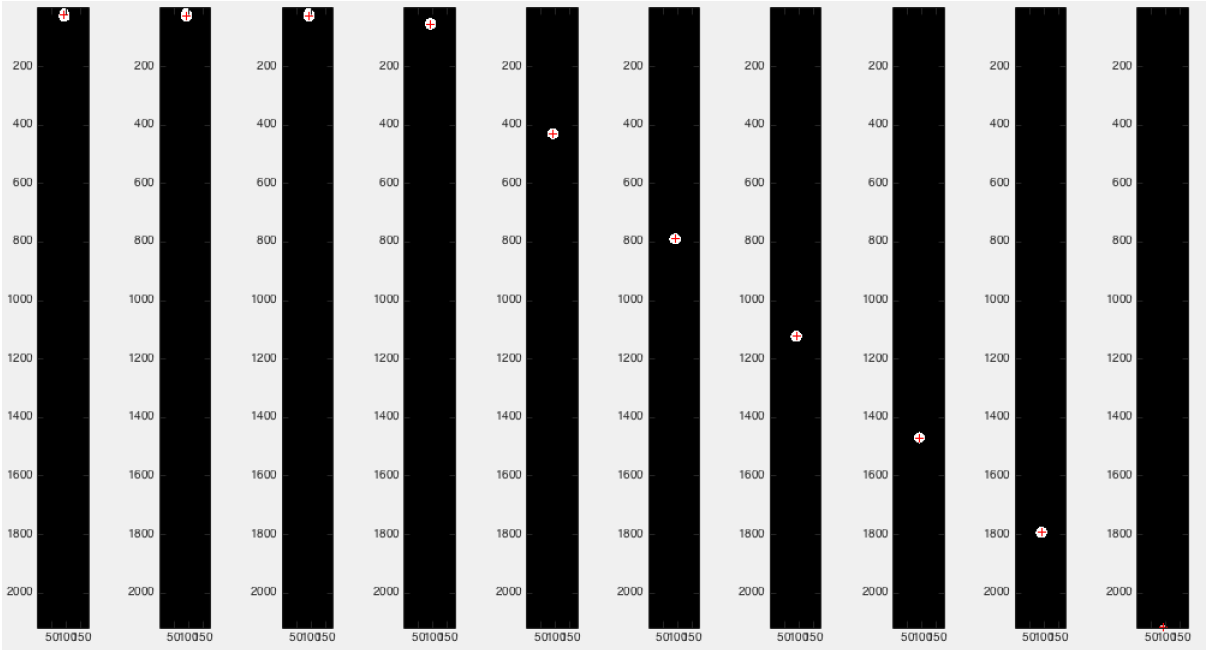

Fig. 25 center of the sphere

To obtain this and the velocities for each sphere we used the following script:

```
% Program computing the trajectory, the velocity and the acceleration of
% the falling sphere.
% Date: 29/04/2015 (author: Nicolas Mazellier, Luca Co & Adelphe Clepin)
%%%%%%%%%%%%%%%%%%%%%%%%%%%%%%%%%%%%%%%%%%%%%%%%%%%%%%%%%%%%%%%%%%%%%%%%%%%

%%%%%%%%%%%%%%%%%%%%%%%%%%%%%%%%%%%%%%%%%%%%%%%%%%%% Calling of parameters
load('Parameters.mat', 'NbImageFall', 'FrameRate', 'pix2m');

%%%%%%%%%%%%%%%%%%%%%%%%%%%%%%%%%%%%%%%%%%%%%%%%%%%% Average Background computation
h = waitbar(0,'Image processing: please wait...');
for indIm = 1 : NbImageFall
    %%%%%%%%%%%%%%%%%%%%%%%%%%%%%%%%%%%%%%%%%%%%%%%%%%%%%%%%%%%%%%%%%%%%%%% Image reading
    file2read = sprintf('Fall/BWImage/Fall%.5d.mat', indIm);
    load(file2read);
    %%%%%%%%%%%%%%%%%%%%%%%%%%%%%%%%%%%%%%%%%%%%%%%%%%%%%%%%%%%%%%%%%%%%%%% Background substracting
    dim = size(BWImage);
    x = [1:dim(1)]*pix2m;
    y = [1:dim(2)]*pix2m;
    [yy, xx] = meshgrid(y, x);

    Sp(indIm) = Integration2D(BWImage, y, x);
    xp(indIm) = Integration2D(xx.*BWImage, y, x)./Integration2D(BWImage, y,
x);
    yp(indIm) = Integration2D(yy.*BWImage, y, x)./Integration2D(BWImage, y,
x);
    waitbar(indIm / NbImageFall);
end
close(h);

time = [0:NbImageFall-1]/FrameRate;

Vpx = DeriveRegul1D(xp, time);
Vpy = DeriveRegul1D(yp, time);
apx = DeriveRegul1D(Vpx, time);
apy = DeriveRegul1D(Vpy, time);

file2save = sprintf('Fall/SphereMotion.mat');
save(file2save,'Sp', 'xp', 'yp', 'Vpx', 'Vpy', 'apx', 'apy');

figure
NbImShow = 10;
indImShow = round(linspace(1, NbImageFall, NbImShow));
for n = 1 : NbImShow
    subplot(1, 10, n)
    file2read = sprintf('Fall/BWImage/Fall%.5d.mat',indImShow(n));
    load(file2read);
    imagesc(BWImage);
    colormap(gray) % To change the colours and the landscape
    axis image % to modify the aspect ratio
    hold on;
    plot(yp(indImShow(n))/pix2m, xp(indImShow(n))/pix2m, '+r')
end

figure
plot(yp, xp, 'o')
axis image

clear all;
```

Once done that for 10 times, we did the avarage velocity between the 10 resulting velocities with this script:

```
x = logspace(log10(1e-4), log10(0.5), 100);
for n = 1 : 15
load([num2str(n) '\Fall\SphereMotion.mat']);
indZero = find(Vpx>0.02, 1);
v(n, :) = interp1((xp(indZero:end)-xp(indZero)), Vpx(indZero:end), x);
end
vmean = mean(v);
vrms = std(v);
```

obtaining our finals plot. We superimpose them to make clearer the differences between the SH sphere and not-covered ones, obtaining respectively a graph for the falls into the water and one for the falls into the glycerol, whose are shown in the 4.1.
Further more it is possible to see the differences between the theoretical velocity that our spheres would have to assume and its trend in a space-velocity graph superimposed with our experimental velocities.

4.3.4 Velocities and terminal velocities: comparision theory and measurements

In order to be able to predict the velocity trend of the spheres, in such a way to know when to stop our measurements , that is when the terminal velocity is reached, we used the following Matlab® script: knowing the density of both sphere and liquid, the factor of view (which is 0.5 m due to the height of the tank) and the diameter of the sphere, it is possible to have a theoretical velocity trend (represented by the green lines in next pictures).

```
function [z, t, vp, Rep, Vpterm, Repterm, Cdterm, Tmeas, dt, fsample] =
TerminalVelocity(rhop, rhof, a, muf, FoV)

% parameter initialisation
g = 9.81;
param = [rhop rhof muf a];

Re      = logspace(log10(1e-2), log10(100000), 1000);
Cd      = DragSphere(Re);
Repterm = interp1(Re.^2.*Cd - (32/3)*(a^3*rhof^2*(rhop/rhof -
1)*9.81/(muf^2)), Re, 0);
Vpterm  = Repterm.*muf./(2*a*rhof);
Cdterm  = 8*a*g*(rhop/rhof - 1)./(3*Vpterm.^2);

tspan   = [0, 2*FoV./Vpterm];
vp0     = 1e-5;
[t, vp] = ode45(@SphereAcceleration, tspan, vp0, [], param);

z       = cumtrapz(t, vp);
Rep     = 2*a*rhof.*vp./muf;
Tmeas   = trapz(z, 1./vp);
dt      = a./Vpterm;
fsample = 1./dt;

figure
plot(z, vp, 'o')
xlabel('$z$ (m)', 'interpreter', 'latex', 'fontsize', 24);
ylabel('$v_p$ (m/s)', 'interpreter', 'latex', 'fontsize', 24);
set(gca,'FontSize',18);
figure
plot(t, vp, 'o')
xlabel('$t$ (s)', 'interpreter', 'latex', 'fontsize', 24);
ylabel('$v_p$ (m/s)', 'interpreter', 'latex', 'fontsize', 24);
set(gca,'FontSize',18);
end
```

It is important to remark that we used for both, glycerol and water, the same properties (findable in Tab.2) for the theoretical script, in order to have a theory based on the exactly same liquids in which experiments are done .

In the picture below (Fig. 26) is possible to see the difference between the velocity trend obtained thanks to the script above and the velocity trend of the average of the 10 experiments for the uncovered sphere, falling in to the glycerol.

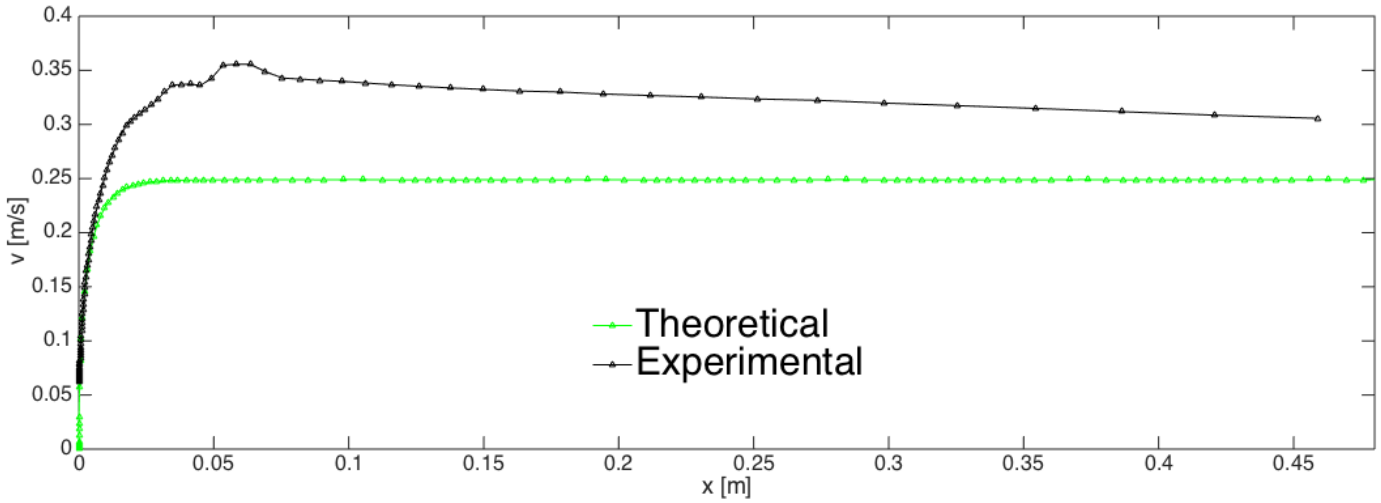

Fig. 26 Overlap of theoretical and experimental velocity for a sphere falling into the glycerol

In this picture we used the properties of water for the theoretical script and we superposed it with the average of the 10 experiments for the uncovered sphere, falling into the water.

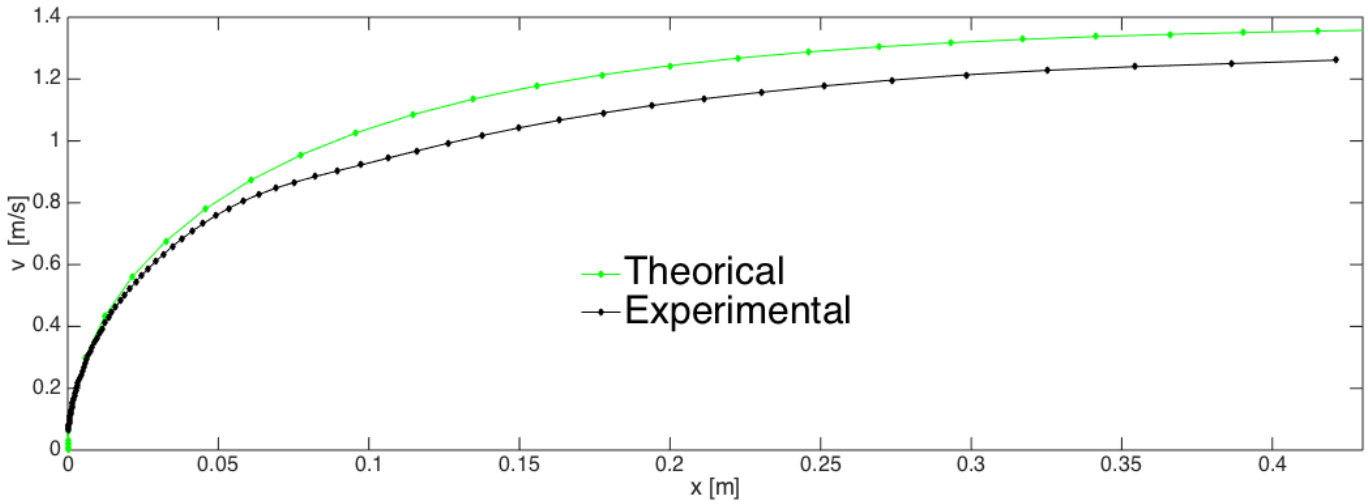

Fig. 27 Overlap of theoretical and experimental velocity for a sphere falling into the water

5 Conclusions

As we saw, the results for both falls into the glycerol and water were not the ones we expected. This probably because the maximum air pressure supportable by air pillars, the same pressure due to (which) the surfaces are SH, has been exceeded. This means that the air trapped between the solid-liquid interface has escaped and we passed from a fakir state to a Wenzel state.
Being then in Wenzel state, the drop tends to stay more blocked than respect in the fakir state or anyway in a normal state where the roughness of the surface has not a hierarchical structure.
We reserve more time to confirm these experiments ,being them in contrast with theory.
This because the transition from a fakir state to the Wenzel state should be, theoretically, when the flow is turbulent or at maximum in transition for turbulence, around a Re number equal to 10^6. Speaking about a sphere falling in to the water, the Re number to pass from laminar to turbulent flow is Re > 10^5. In our experiments we never passed Re = 20000, and then we should not have any negative effects related to the maximum air pressure supportable from air pillars. Maybe the problems are related not to the SH surfaces in general but to the SH coating we used, or maybe to the process we adopted to coated the spheres.
Furthermore we will make several new experiments, in order to see and analyze the results, to be able to understand better if the negative effects due to the SH coating are given by our mstake or if air pillars presents in the SH surfaces do not support the pression generated from the fluid which flows above them already for Re > 10^5.

6 Future applications and environmental impact

In light of their slip properties and the drag reduction for a body moving in a fluid, the first application for SH surfaces is obviously on the hull of ships.
The benefits expected are tremendous; for example, in the maritime transport sector, skin friction drag contributes to over 60% of the total drag for a cargo ship and 80% for a tanker. Lowering drag by even a small amount would have a global impact on energy saving and greenhouse gas reduction.
If we consider their property on light of static and semi-dynamic applications, SH surfaces have many applications.
They can prevent the formation of ice on aircraft wings, the electrical cables, the wind turbines, and all other components affected to this problem.
Improving the rolling of the liquid on the surface can be extremely important in many cases:
In power plants and industrial installations those base their operations on the transport of heat, in cases where the condensation of the vapor can lead to a reduction in the efficiency.
In self-cleaning surfaces, in which the rolling of the droplets allows to incorporate and remove contaminating particles which, having dimensions greater than those of the surface structures, do not penetrate into the roughness.
In the glass of the windshield where the adhesion of raindrops can compromise the visibility.
Of course, based on the properties of SH surfaces, many other engineering applications can be found, according to the problem to solve and the work to do, by technological improvement.
Taking a look to that problems which are not strictly engineering, SH surfaces could have applications that would ensure energy savings and better quality in everyday life. For example, a big problem that we can find in the poorest countries affected by water scarcity, is the igenic condictions of public facilities. Considering the static and semi-dynamics properties of SH surfaces, we can hipotise to build toilets in such a way that dirt could slip away easily, and the water needed for each wash would decrease substantially.

REFERENCES

1. Alessandro Bottaro : Superhydrophobic surfaces for drag reduction , 2014
2. Unimore, nanolab : Superfici Nanostrutturate e Nanotribologia , 2013
3. Jonathan P. Rothstein: Slip on Superhydrophobic Surfaces , 2009
4. Liangliang Cao : Superhydrophobic surface. Design, fabrication, and applications, University of Pittsburgh, 2010
5. Elena Celia, Thierry Darmanin, Elisabeth Taffin de Givenchy, Sonia Amigoni, Frédéric Guittard : Recent advances in designing superhydrophobic surfaces , July, 2013
6. Gareth H. Mckinley : The unsteady motion of a sphere in a viscoelastic fluid, MIT,1994

RINGRAZIAMENTI

Desidero ringraziare il Prof. Alessandro Bottaro ed il Prof. Nicolas Mazellier per avere unito le loro forze ed avermi permesso di svolgere questa esperienza con il supporto di entrambi.
Desidero ringraziare il Prof. Alessandro Bottaro per non essersi fermato a farmi da professore solo per il suo esame, ma per aver contribuito in questi anni ad aprire i miei orizzonti e ampliare le mie visioni.
Ringrazio i miei genitori e la mia famiglia per le opportunità che da sempre mi danno, alle quali grazie sono qui ora.
Ringrazio i miei genitori per aver sempre combattuto su ogni centimetro, ed avermi insegnato a farlo.
Saluto mio Zio Luciano, al quale prometto, il suo nome non sarà dimenticato.